

See discussions, stats, and author profiles for this publication at: <https://www.researchgate.net/publication/259969267>

# Highly Mobile Ions: Low-Temperature NMR Directly Probes Extremely Fast Li<sup>+</sup> Hopping in Argyrodite-Type Li<sub>6</sub>PS<sub>5</sub>Br

ARTICLE *in* JOURNAL OF PHYSICAL CHEMISTRY LETTERS · JULY 2013

Impact Factor: 7.46 · DOI: 10.1021/jz401003a

---

CITATIONS

17

---

READS

78

4 AUTHORS, INCLUDING:



Martin Wilkening

Graz University of Technology

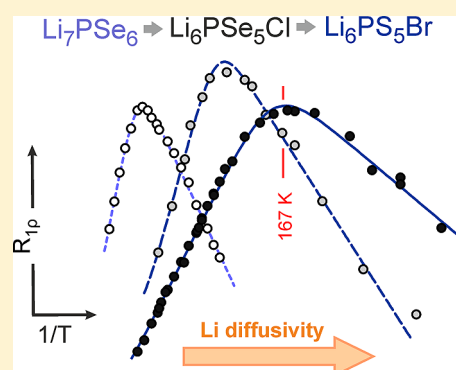
119 PUBLICATIONS 1,564 CITATIONS

SEE PROFILE

Highly Mobile Ions: Low-Temperature NMR Directly Probes Extremely Fast  $\text{Li}^+$  Hopping in Argyrodite-Type  $\text{Li}_6\text{PS}_5\text{Br}$ Viktor Epp,<sup>\*,†</sup> Özgül Gün,<sup>‡</sup> Hans-Jörg Deiseroth,<sup>‡</sup> and Martin Wilkening<sup>\*,†</sup><sup>†</sup>Christian Doppler Laboratory for Lithium Batteries, and Institute for Chemistry and Technology of Materials, Graz University of Technology, Stremayrgasse 9, 8010 Graz, Austria<sup>‡</sup>Anorganische Chemie, University of Siegen, Adolf-Reichwein-Straße 2, 57068 Siegen, Germany

## Supporting Information

**ABSTRACT:** The development of safe and long-lasting all-solid-state lithium-ion batteries needs electrolytes with exceptionally good transport properties. Here, we report on the combination of several solid-state nuclear magnetic resonance (NMR) techniques which have been used to precisely probe short-range as well as long-range  $\text{Li}^+$  dynamics in  $\text{Li}_6\text{PS}_5\text{Br}$  from an atomic-scale point of view. NMR data clearly reveal an extraordinary high Li diffusivity. This manifests in so-called diffusion-induced spin–lattice relaxation NMR rate peaks showing up at temperatures as low as 260 K. From a quantitative point of view, at ambient temperature the Li jump rate is of the order of  $10^9 \text{ s}^{-1}$  which corresponds to a  $\text{Li}^+$  conductivity in order of  $10^{-3}$  to  $10^{-2} \text{ S/cm}$ , thus, indicating “liquid-like”  $\text{Li}^+$  diffusion behavior in  $\text{Li}_6\text{PS}_5\text{Br}$ .

**SECTION:** Kinetics and Dynamics

Since the discovery of ionic conduction in solids many decades ago, the research field, which is frequently known as *solid state ionics* today, has emerged to be one of the most important subdisciplines of physical chemistry, in particular, and materials science, in general. Currently, this ongoing progress is additionally driven by the increasing demand to realize advanced and energy-dense electrochemical storage systems that need fast ion conductors.

Looking toward improved lithium-ion batteries<sup>1–4</sup> for, for example, electric vehicles as well as for storing energy from renewable but intermittent sources, new materials with extraordinary transport properties have to be developed, thoroughly characterized, and tested. To go beyond today's commercially available systems, which mostly rely on flammable liquid electrolytes, more than ever before, *solid* electrolytes<sup>5</sup> are indispensable to guarantee both safety and reliability as well as a long life of a rechargeable battery.

Besides thermal and electrochemical stability, a powerful solid electrolyte, which conducts lithium ions between the negatively charged anode and the positive cathode, needs to have an Li ion conductivity higher than  $10^{-3} \text{ S/cm}$  near room temperature. So far, only a few crystalline solids are known<sup>5–12</sup> that meet these requirements. Once promising candidates are found, Li transport parameters have to be precisely and reliably measured.<sup>13</sup> However, in the case of lithium the pool of methods is rather limited. For example, because there is no suitable long-living isotope known, the well-known radio tracer method cannot be applied. Conductivity spectroscopy needs careful postpreparation of the sample and might suffer from

porosity, grain boundary resistances, and electrode effects.<sup>14</sup> Nuclear magnetic resonance (NMR) spectroscopy,<sup>15–20</sup> however, which takes advantage of the superb receptivity of the  $^7\text{Li}$  nucleus (spin-3/2), represents an atomic-scale, nondestructive, and even contactless method to be used for this purpose. Moreover, the combination of complementary time-domain NMR techniques allows probing Li diffusion parameters over a large dynamic range, covering in the best case more than 10 decades.<sup>19,21,22</sup>

We report on an example par excellence where relaxation NMR was used to directly probe Li jump rates  $1/\tau$  and activation energies  $E_a$  in argyrodite-type cubic  $\text{Li}_6\text{PCh}_5\text{X}$  ( $\text{Ch} = \text{S, Se}$ ;  $\text{X} = \text{Cl, Br}$ ),<sup>14,23,24</sup> representing a new class of highly conducting solid electrolytes. It turned out that polycrystalline  $\text{Li}_6\text{PS}_5\text{Br}$  belongs, as yet, to one of the fastest solid Li conductors investigated by Li NMR. The results even exceed those recently reported for an ultrafast jump diffusion process in  $\text{Li}_{12}\text{Si}_7$ .<sup>25</sup> Finally, by systematically comparing the results of different members of the  $\text{Li}_6\text{PS}_5\text{Br}$  family, the measurements helped us to understand how anion substitution may improve cation diffusivity – a general concept that is extremely advantageous to tailor transport properties. Let us note that, even today, a knowledge-based and target-oriented development of functional materials, in the true sense of the word, has been documented extremely rarely.

Received: May 14, 2013

Accepted: June 11, 2013

Published: June 11, 2013

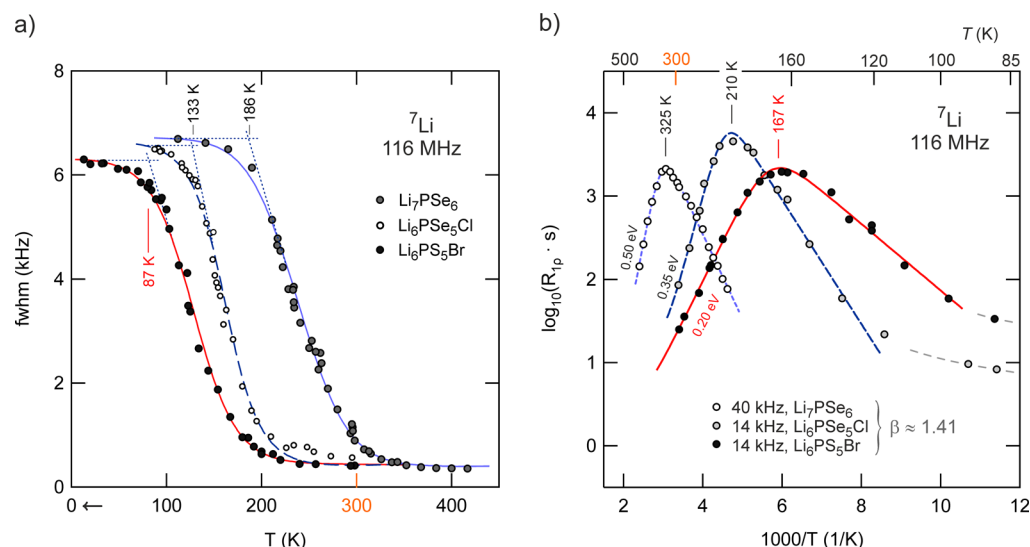


**Figure 1.** (a) Temperature dependence of the  $^7\text{Li}$  NMR line widths (full width at half-maximum) of three selected Li-argyrodites. Data for  $\text{Li}_7\text{PSe}_6$  were taken from ref 32. Lines are to guide the eye. Dotted lines indicate the determination of the onset of motion-induced line narrowing. A value of 87 K, which is obtained for  $\text{Li}_6\text{PS}_5\text{Br}$ , indicates extremely fast hopping processes. (b) Arrhenius plot of the corresponding  $^7\text{Li}$  SLR  $\rho$  NMR rates recorded at the locking frequencies indicated. Here, at the peak maximum, the Li jump rate is at least  $10^5 \text{ s}^{-1}$ . The lines represent fits according to a modified BPP relaxation model,<sup>13,36,37</sup> taking into account its asymmetry by introducing the parameter  $\beta$ . The farther the diffusion-induced NMR relaxation peak is shifted toward lower  $T$ , the faster Li exchange and the smaller the activation energy turns out. The latter is directly given by the slope of the respective high-temperature flank. In summary, Li diffusion drastically increases in the following order:  $\text{Li}_7\text{PSe}_6 < \text{Li}_6\text{PSe}_5\text{Cl} < \text{Li}_6\text{PS}_5\text{Br}$ . See the text for further details.

The Li-argyrodites, with natural Li abundance ( $^7\text{Li}$  92.5%,  $^6\text{Li}$  7.2%), were prepared by solid-state synthesis; details of sample preparation are described elsewhere.<sup>14</sup> To protect the polycrystalline powder samples permanently from any traces of moisture they were carefully fire-sealed in glass ampoules.  $^7\text{Li}$  NMR line shapes and spin–lattice relaxation (SLR) measurements in both the laboratory and rotating frame of reference were recorded on a digital Avance III NMR spectrometer that is connected to a shimmed cryo magnet with a nominal magnetic field of 7 T. (See the Supporting Information for further experimental details.) Because of the high diffusivity of the Li ions in  $\text{Li}_6\text{PS}_5\text{Br}$  the NMR measurements had to be partly performed at cryogenic temperatures as low as 13 K. For that purpose a special probe designed by Bruker was employed. While line shapes were recorded with a single pulse, SLR NMR rates were acquired using the saturation recovery technique<sup>17,26</sup> and a spin-lock pulse sequence,<sup>26–28</sup> respectively.

First insights into Li dynamics of crystalline solids can be deduced from the motion-induced narrowing of static Li NMR spectra recorded at different temperatures.<sup>29,30</sup> At sufficiently low  $T$ , that is, in the so-called rigid-lattice regime, the Li jump rate  $1/\tau$  is much smaller than the spectral width of the usually dipolarly broadened Gaussian NMR central line. With increasing temperature, however, Li exchange processes become faster, and  $1/\tau$  reaches values being comparable to the spectral width. The associated averaging of dipole–dipole interactions results in a motionally narrowed, in many cases, Lorentzian NMR central line.<sup>31</sup> This behavior is also observed in the present case. For comparison, in Figure 1a, the NMR line widths (full width at half-maximum) for three selected Li-argyrodites are plotted versus temperature. While onset of motional narrowing (MN) for  $\text{Li}_7\text{PSe}_6$  significantly starts at  $T_{\text{MN}} = 186 \text{ K}$ ,<sup>32</sup> the corresponding curve of  $\text{Li}_6\text{PSe}_5\text{Cl}$  is clearly shifted toward lower temperature yielding  $T_{\text{MN}} = 133 \text{ K}$ . This value is comparable to that found recently for the ultrafast

diffusion process in polycrystalline  $\text{Li}_{12}\text{Si}_7$ . At the onset point of the narrowing curve the jump rate  $1/\tau$  is expected to be on the order of  $10^3 \text{ s}^{-1}$ . Most importantly, a further shift is observed for  $\text{Li}_6\text{PS}_5\text{Br}$ , resulting in an extremely low onset temperature of  $T_{\text{MN}} = 87 \text{ K}$  (Figure 1a). The results nicely corroborate those reported by Eckert and coworkers,<sup>7</sup> who recorded NMR spectra down to 130 K, as well as confirm the data presented by Koch.<sup>33</sup> To verify such ultrafast diffusion processes, we measured diffusion-induced  $^6\text{Li}$  and  $^7\text{Li}$  SLR NMR rates at different frequencies and over a broad temperature range.

Provided SLR is solely induced by diffusion processes, the NMR SLR rate  $R_{1\rho}$  passes through a maximum on a  $\log(R_{1\rho})$  versus  $1/T$  plot.<sup>13,17,34</sup> When  $R_{1\rho}$  reaches its maximum value the mean correlation rate, being almost identical to the Li jump rate  $1/\tau$ , was on the order of the Larmor ( $\omega_0$ ) or locking frequency ( $\omega_1$ ) used to sample the NMR rates.<sup>13,17</sup> Because  $\omega_0$  is in the megahertz range and  $\omega_1$  is on the order of kilohertz, complementary SLR NMR experiments are sensitive to motional processes covering a quite large time scale. Let us first discuss those carried out at comparable locking frequencies of  $\omega_1/2\pi = 45$  and 14 kHz, respectively (see Figure 1b).<sup>35</sup> While  $\text{Li}_7\text{PSe}_6$  reveals an asymmetric rate peak showing up at  $T_{\text{max}} = 325 \text{ K}$ , that of the Cl-containing argyrodite shows up at 210 K, indicating greatly improved Li diffusion; in the case of rotating frame SLR  $\rho$ , at  $T_{\text{max}}$  the jump rate is given by  $1/\tau(T_{\text{max}}) \approx 2\omega_1$ ,<sup>13,17</sup> thus, being on the order of  $10^6 \text{ s}^{-1}$ . In perfect agreement with the line width measurements (Figure 1a), the rate peak  $R_{1\rho}(1/T)$  of  $\text{Li}_6\text{PS}_5\text{Br}$ , which was recorded at  $\omega_1/2\pi = 14 \text{ kHz}$ , is shifted toward even lower  $T$  yielding  $T_{\text{max}} = 167 \text{ K}$  (Figure 2b). For comparison, considering other fast ion conductors studied, a value on the order of  $10^5$  jumps per second is usually found slightly below room temperature.<sup>21</sup> Here the shift of more than 100 K toward lower  $T$  unequivocally classifies  $\text{Li}_6\text{PS}_5\text{Br}$  as an electrolyte with fast Li exchange processes.

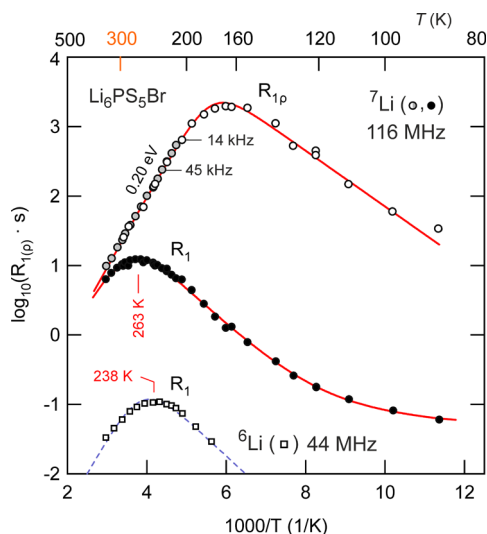


**Figure 2.** Arrhenius plot of the  $^7\text{Li}$  NMR relaxation rates  $R_1$  and  $R_{1\rho}$  of polycrystalline  $\text{Li}_6\text{PS}_5\text{Br}$  measured in both the rotating frame (see Figure 1b) and laboratory frame of reference. Solid lines represent a joint fit being based on the BPP model (see text). For comparison, the diffusion-induced  $^6\text{Li}$  SLR NMR rates recorded at 44 MHz are also included. Li SLR NMR rate maxima, showing up at 263 and 238 K, that is, well below room temperature, point to extremely fast, translational Li ion motions with jump rates of the order of  $10^9 \text{ s}^{-1}$ , that is, residence times as low as 1 ns.

At room temperature, the jump rate of  $\text{Li}_6\text{PS}_5\text{Br}$  is expected to reach even larger values. Indeed, SLR NMR measurements performed at a resonance frequency of 116 MHz reveal a diffusion-induced rate peak  $R_{1\rho}(1/T)$  passing through its maximum at  $T_{\text{max}} = 263 \text{ K}$  (Figure 2). This has been corroborated by complementary  $^6\text{Li}$  measurements carried out at 44 MHz yielding  $T_{\text{max}} = 238 \text{ K}$  (see also Figure 2). With  $1/\tau(T_{\text{max}}) \approx \omega_1$ , being valid for SLR NMR in the *laboratory frame* of reference,<sup>17</sup> this yields  $1/\tau(238 \text{ K}) = 2.8 \times 10^8 \text{ s}^{-1}$  and  $1/\tau(263 \text{ K}) = 7.3 \times 10^8 \text{ s}^{-1} \approx 10^9 \text{ s}^{-1}$ , respectively. Thus, well below room temperature the mean residence time of a Li ion is close to 1 ns. To our knowledge this is so far one of the fastest solid-state diffusion processes probed by time-domain  $^6,7\text{Li}$  NMR relaxometry. For comparison, in  $\text{Li}_{12}\text{Si}_7$ , the  $R_1(1/T)$  rate peak shows up at much higher temperatures (viz.  $T_{\text{max}} = 400 \text{ K}$ ) when measured at 77.7 MHz.<sup>25</sup>

The jump rates derived from SLR NMR can be converted into conductivity values according to the Einstein–Smoluchowski equation and the Nernst–Einstein equation.<sup>38</sup> The first interrelates  $1/\tau$  with the self-diffusion coefficient: assuming 3D diffusion and a jump distance of  $2.5 \text{ \AA}$ , which is a very reasonable value in the present case,<sup>39</sup> we obtain  $D_{263\text{K}} = a^2/(6\tau) = 7.6 \times 10^{-8} \text{ cm}^2 \text{ s}^{-1}$  (in a relatively theory-independent way). Disregarding any correlation effects, by means of the Nernst–Einstein equation,  $D_{263\text{K}}$  can roughly be converted into a conductivity value  $\sigma$ . Here a mean residence time of 1 ns corresponds to  $\sigma$  in the order of  $\sigma \approx 10^{-2} \text{ S/cm}$ , clearly illustrating extremely mobile lithium ions in polycrystalline  $\text{Li}_7\text{PS}_6\text{Br}$  (see below). Certainly, this conversion should be regarded as a rough estimate because relaxation NMR and conductivity spectroscopy sense different kinds of correlation functions.<sup>40,41</sup>

To understand the motion-induced  $^7\text{Li}$  SLR NMR rates of  $\text{Li}_7\text{PSe}_6$ ,  $\text{Li}_6\text{PSe}_5\text{Cl}$ , and  $\text{Li}_6\text{PS}_5\text{Br}$  in more detail, we used modified BPP-type<sup>42</sup> spectral density functions  $J(\omega_0, \tau_c)$  that are based on exponential motional correlation functions<sup>17,42</sup>  $G(t')$  to describe the temperature dependence of  $R_1(1/T)$  and  $R_{1\rho}(1/T)$ , respectively.<sup>13,25,34</sup> The correlation time  $\tau_c$  is within a factor of  $2^{17}$  identical to the Li residence time  $\tau = \tau_0 \exp(-E_a/(k_B T))$ ; here  $E_a$  denotes the activation energy and  $k_B$  is Boltzmann's constant.

The Lorentzian-shaped function  $J$ , which is directly proportional to  $R_1$  and  $R_{1\rho}$ , can be derived from  $G$  by Fourier transformation.<sup>17,43</sup> In the case of a 3D diffusion process, we have  $J \propto \tau$  at high temperatures, that is, in the limit  $\omega_{0(\rho)}\tau \ll 1$ , and  $J \propto \tau^{-1}\omega_{0(\rho)}^{-\beta}$  (with  $1 < \beta \leq 2$ ) in the low  $T$  limit where  $\omega_{0(\rho)}\tau \gg 1$  holds.<sup>17,34</sup> Original BPP-type behavior<sup>36</sup> does not take into account correlation effects and predicts  $\beta = 2$  leading to symmetric relaxation rate peaks.<sup>17,44</sup> Asymmetric peaks are usually found for structurally complex or even disordered ion conductors.<sup>6,13,34</sup> Such materials reveal a broad range of short-range and long-range motional processes that are affected by correlation effects<sup>45</sup> resulting from, for example, Coulomb interactions.<sup>46</sup> In the present case, the  $R_{1\rho}(1/T)$  fits yield an asymmetry parameter  $\beta_\rho \approx 1.4$  (Figure 1b), while  $\beta \approx 1.5$  is found for the  $^7\text{Li}$  NMR (and  $^6\text{Li}$  NMR) rates recorded in the laboratory frame of reference (see Figure 2). The small difference in  $\beta$  points to slightly differing correlation effects affecting the SLR NMR rates, which are per se sensitive to Li motions on different time scales.<sup>34</sup>

It is clearly evident from Figure 1b that  $E_a$ , which can be independently deduced from the slope of the high- $T$  flank, decreases from  $\sim 0.5 \text{ eV}$  in steps of  $0.15 \text{ eV}$ . This result is in excellent agreement with the shift of the rate peaks observed: the smaller  $E_a$ , the faster Li diffusion becomes. Thus, Li exchange drastically increases in the following order:  $\text{Li}_7\text{PSe}_6$  ( $\approx \text{Li}_7\text{PS}_6$ )  $< \text{Li}_6\text{PSe}_5\text{Cl} < \text{Li}_6\text{PS}_5\text{Br}$ . Let us note that  $\text{Li}_7\text{PSe}_6$ , investigated in ref 32 in detail, is expected to show very similar diffusion parameters as the S-analogue  $\text{Li}_7\text{PS}_6$ . The value found for  $\text{Li}_6\text{PSe}_5\text{Cl}$  ( $0.35 \text{ eV}$ ) is in good agreement with the one calculated by Rao et al. characterizing the 3D long-range pathway network.<sup>23</sup>

The lowest value,  $E_a = 0.20(1) \text{ eV}$  ( $200 \text{ K} < T < 330 \text{ K}$ , see Figure 2), is also found when the NMR peaks  $R_{1\rho}(1/T)$  and  $R_1(1/T)$  of  $\text{Li}_6\text{PS}_5\text{Br}$  are analyzed in terms of a global fit (solid lines in Figure 2), that is, linking the fitting parameters such as  $\omega_0$ , the activation energies, and coupling constants. In the present case, however, the best fit is obtained when  $\beta \neq \beta_\rho$  (see above) and  $1/\tau_0$  of SLR NMR is independent of that used to parametrize the  $R_{1\rho}(1/T)$  peak. It is worth noting that nondiffusive background relaxation, see the SLR NMR rates of Figure 2, which were recorded below  $120 \text{ K}$ , were taken into account by an appropriate power law:  $R_1 \propto T^\kappa$  with  $\kappa \approx 2$ . Such effects, which are also seen in Figure 1b, presumably represent SLR induced by lattice vibrations or by coupling of the Li spins with traces of paramagnetic impurities. Moreover, from many different runs of the global fit procedure it turned out that it is useful to replace  $\omega_1 = 14 \text{ kHz} \times 2\pi$  with a slightly larger value of  $\omega_{\text{eff}} = 1.4 \omega_1$ . Here the factor of 1.4 takes into account local magnetic fields in the order of the locking field.

For comparison, the fitting results obtained are listed in Table 1. Interestingly, the  $R_{1\rho}$  data seem to underestimate the Arrhenius prefactor, leading to  $\tau_0 = 6(2) \times 10^{-12} \text{ s}$ , while the  $R_1(1/T)$  peak yields  $\tau_0 = 2(1) \times 10^{-13} \text{ s}$ . The latter value, whose inverse agrees with the typical range of phonon frequencies, is corroborated by analyzing the  $^6\text{Li}$   $R_1(1/T)$  rate peak, which is best characterized by  $\tau_0 = 3(1) \times 10^{-13} \text{ s}$ .



**Table 1. Results ( $E_a$ ,<sup>b</sup>  $\beta_{(p)}$ ,  $\tau_0$ , and the pre-factor  $C^c$ ) of the overall SLR NMR Fit Shown in Figure 2 (solid lines)<sup>a</sup>**

	$E_a^b$	$C^c$	$\beta_{(p)}$	$\tau_0$
$R_1$ ( $^7\text{Li}$ )	0.20(1) eV	$5.8(1) \times 10^9 \text{ s}^{-2}$	1.54	$2(1) \times 10^{-13} \text{ s}$
$R_{1p}$ ( $^7\text{Li}$ )			1.36	$6(1) \times 10^{-12} \text{ s}$
$R_1$ ( $^6\text{Li}$ )	0.20(3) eV	$2(1) \times 10^7 \text{ s}^{-2}$	1.53	$3(1) \times 10^{-13} \text{ s}$

<sup>a</sup>The fit was carried out using  $\omega_{\text{eff}} = 1.4 \omega_1$  with  $\omega_1 = 14 \text{ kHz} \times 2\pi$ ,  $\omega_0(^7\text{Li}) = 116 \text{ MHz} \times 2\pi$ , and  $\omega_0(^6\text{Li}) = 44 \text{ MHz} \times 2\pi$ . <sup>b</sup>This value refers to the slope of the high- $T$  flank of the SLR NMR peaks. <sup>c</sup>The prefactor  $C$  interrelates  $J(\omega_0, \tau_c)$  with the relaxation rate  $R_1$ . Values ranging from  $10^9$  to  $10^{10} \text{ s}^{-2}$  correspond to the square of typical  $^7\text{Li}$  quadrupole coupling constants.<sup>31</sup> Note that the quadrupole moment of  $^6\text{Li}$  is by a factor of 50 smaller than that of  $^7\text{Li}$ ; therefore, for  $^6\text{Li}$  NMR, the dipolar contributions play a non-negligible role.

Thus, describing (long-range) Li diffusion in  $\text{Li}_6\text{PS}_5\text{Br}$  with a single Arrhenius relation, the jump rate  $\tau(T)$  is given by  $\tau = 3(1) \times 10^{-13} \text{ s} \cdot \exp(-0.20(2) \text{ eV}/(k_B T))$ . According to that result, at  $T = 125 \text{ K}$ , that is, at the temperature of the inflection point of the NMR motional narrowing curve of  $\text{Li}_6\text{PS}_5\text{Br}$  (see Figure 1b), the jump rate  $1/\tau$  should be on the order of  $3.5 \times 10^4 \text{ s}^{-1}$ . Indeed, with the rigid lattice line width  $\Delta\nu_{\text{rl}} = 6 \text{ kHz}$ , the estimation  $1/\tau \approx \Delta\nu_{\text{rl}} \times 2\pi$  yields  $3.9 \times 10^4 \text{ s}^{-1}$ . Certainly, this agreement does not rule out the presence of other, quite different and temperature-dependent diffusion processes. In particular, while activation energies determined in the limit  $\omega_0 \tau \ll 1$  are generally compared with those from dc-conductivity probing long-range ion transport,<sup>17,34</sup> the low- $T$  flank of the  $R_{1p}(1/T)$  rate peak is influenced by short-range motional processes characterized by much smaller activation energies;<sup>34</sup> here, this is 0.08(2) eV for  $\text{Li}_6\text{PS}_5\text{Br}$  and 0.15(2) eV for the Cl-analogue; cf. also results from theoretical studies including also I-containing compounds.<sup>23,39</sup>

Finally, it is highly useful to compare the absolute values of the purely diffusion-induced  $^6\text{Li}$  (spin-1) NMR rates in the limit  $\omega_0 \tau \ll 1$  with those of the corresponding  $^7\text{Li}$  (spin-3/2) NMR rate peak. For dipolar interactions being responsible for SLR NMR, the ratio  $R_1(^6\text{Li})/R_1(^7\text{Li}) = r$  is expected to be on the order of two, while for quadrupolar relaxation  $r$  should be on the order of  $10^{-4}$ .<sup>47</sup> Experimentally we found  $5.3(2) \times 10^{-3}$  pointing to a quadrupolar mechanism influencing  $^7\text{Li}$  NMR spin-lattice relaxation here.

In conclusion, among the Li-argyrodites studied here,  $\text{Li}_6\text{PS}_5\text{Br}$  turned out to be a material with an exceptionally high Li diffusivity. The corresponding long-range jump process is characterized by a hopping activation energy of only 0.2 eV as deduced from the various temperature-variable NMR SLR measurements. This extraordinary feature manifests in (laboratory frame) SLR NMR rate peaks showing up at temperatures as low as 260 K. From a quantitative point of view, at room temperature, this yields a Li jump rate of  $10^9 \text{ s}^{-1}$ , which corresponds to an  $\text{Li}^+$  conductivity on the order of  $10^{-3}$  to  $10^{-2} \text{ S/cm}$ , thus indicating “liquid-like” diffusion behavior comparable to, for example, the interlayer process in  $\text{Li}_3\text{N}$ .<sup>48</sup> The activation energy and the estimated ionic conductivity from SLR NMR are in agreement with results deduced from previous and recent conductivity studies.<sup>7,23,49</sup> Let us note that in the limit of  $\omega_0 \tau \ll 1$ , SLR NMR is expected to yield activation energies being comparable to those characterizing long-range ion transport, while on the low- $T$  side of a given NMR relaxation peak, localized, that is, short-range, Li motional processes are probed.<sup>17,34</sup>

The high Li diffusivity found makes the development of safe and long-lasting all-solid-state lithium batteries feasible. It might be understood by comparing the results from the three different samples studied: because Li diffusivity increases from  $\text{Li}_7\text{PSe}_6$  to  $\text{Li}_6\text{PSe}_5\text{Cl}$  (and  $\text{Li}_6\text{PS}_5\text{Br}$ ), the structural mismatch and strain generated by substitution of a large halogen ion for, for example, selenium, seems to be highly relevant when a high Li mobility needs to be achieved. Moreover, the larger Li diffusivity of  $\text{Li}_6\text{PS}_5\text{Br}$  against  $\text{Li}_6\text{PSe}_5\text{Cl}$  might be attributed to the combination of anions with different polarizabilities. In summary, the present example illustrates how anion substitution can be used as a tool to successfully manipulate cation diffusivity in a crystalline solid.

## ■ ASSOCIATED CONTENT

### Supporting Information

Cf. for experimental details including information on the equipment used, the measurement conditions chosen, and the pulse sequences applied to record the SLR NMR data. This material is available free of charge via the Internet at <http://pubs.acs.org>.

## ■ AUTHOR INFORMATION

### Corresponding Author

\*E-mail: [viktor.epp@tugraz.at](mailto:viktor.epp@tugraz.at); [wilkening@tugraz.at](mailto:wilkening@tugraz.at).

### Notes

The authors declare no competing financial interest.

## ■ ACKNOWLEDGMENTS

We thank G. Schmidt (Bruker, Karlsruhe (Germany)) for his help with setting up the NMR spectrometer at the TU Graz. Financial support by the Austrian Federal Ministry of Economy, Family and Youth and the Austrian National Foundation for Research, Technology and Development as well as by the Deutsche Forschungsgemeinschaft (DFG) is highly appreciated (DFG Forschergruppe 1277, grant no.: WI3600 4-1/4-2).

## ■ REFERENCES

- (1) Aricò, A. S.; Bruce, P.; Scrosati, B.; Tarascon, J.-M.; Schalkwijk, W. V. Nanostructured Materials for Advanced Energy Conversion and Storage devices. *Nat. Mater.* **2005**, *4*, 366–377.
- (2) Tarascon, J. M.; Armand, M. Issues and Challenges Facing Rechargeable Lithium Batteries. *Nature* **2001**, *414*, 359–367.
- (3) Bruce, P. G.; Scrosati, B.; Tarascon, J.-M. Nanomaterials for Rechargeable Lithium Batteries. *Angew. Chem., Int. Ed.* **2008**, *47*, 2930–2946.
- (4) Armand, M.; Tarascon, J.-M. Building Better Batteries. *Nature* **2008**, *451*, 652–657.
- (5) Knauth, P. Inorganic Solid Li Ion Conductors: An Overview. *Solid State Ion.* **2009**, *180*, 911–916.
- (6) Buschmann, H.; Dölle, J.; Berendts, S.; Kuhn, A.; Bottke, P.; Wilkening, M.; Heitjans, P.; Senyshyn, A.; Ehrenberg, H.; Lotnyk, A.; Duppel, V.; Kienle, L.; Janek, J. Structure and Dynamics of the Fast Lithium Ion Conductor “ $\text{Li}_7\text{La}_3\text{Zr}_2\text{O}_{12}$ ”. *Phys. Chem. Chem. Phys.* **2011**, *13*, 19378–19392.
- (7) Deiseroth, H.-J.; Kong, S.-T.; Eckert, H.; Vannahme, J.; Reiner, C.; Zaiss, T.; Schlosser, M.  $\text{Li}_6\text{PS}_5\text{X}$ : A Class of Crystalline Li-Rich Solids With an Unusually High  $\text{Li}^+$  Mobility. *Angew. Chem., Int. Ed.* **2008**, *47*, 755–758.
- (8) Hayashi, A.; Tatsumisago, M. Recent Development of Bulk-type Solid-state Rechargeable Lithium Batteries with Sulfide Glass-Ceramic Electrolytes. *Electron. Mater. Lett.* **2012**, *8*, 199–207.
- (9) Murugan, R.; Thangadurai, V.; Weppner, W. Fast Lithium Ion Conduction in Garnet-Type  $\text{Li}_7\text{La}_3\text{Zr}_2\text{O}_{12}$ . *Angew. Chem., Int. Ed.* **2007**, *46*, 7778–7781.

- (10) Kamaya, N.; Homma, K.; Yamakawa, Y.; Hirayama, M.; Kanno, R.; Yonemura, M.; Kamiyama, T.; Kato, Y.; Hama, S.; Kawamoto, K.; Mitsui, A. A Lithium Superionic Conductor. *Nat. Mater.* **2011**, *10*, 682–686.
- (11) Takada, K.; Tansho, M.; Yanase, I.; Inada, T.; Kajiyama, A.; Kouguchi, M.; Kondo, S.; Watanabe, M. Lithium Ion Conduction in  $\text{LiTi}_2(\text{PO}_4)_3$ . *Solid State Ion.* **2001**, *139*, 241–247.
- (12) Hayamizu, K.; Aihara, Y. Lithium Ion Diffusion in Solid Electrolyte  $(\text{Li}_2\text{S})_x(\text{P}_2\text{S}_5)_3$  Measured by Pulsed-Gradient Spin-echo  $^7\text{Li}$  NMR Spectroscopy. *Solid State Ion.* **2013**, *238*, 7–14.
- (13) Kuhn, A.; Narayanan, S.; Spencer, L.; Goward, G.; Thangadurai, V.; Wilkening, M. Li Self-diffusion in Garnet-type  $\text{Li}_x\text{La}_3\text{Zr}_2\text{O}_{12}$  as Probed Directly by Diffusion-induced  $^7\text{Li}$  Spin-lattice Relaxation NMR Spectroscopy. *Phys. Rev. B* **2011**, *83*, 094302/1–094302/11.
- (14) Deiseroth, H.-J.; Maier, J.; Weichert, K.; Nickel, V.; Kong, S.-T.; Reiner, C.  $\text{Li}_7\text{PS}_6$  and  $\text{Li}_6\text{PS}_5\text{X}$  (X: Cl, Br, I): Possible Three-dimensional Diffusion Pathways for Lithium Ions and Temperature Dependence of the Ionic Conductivity by Impedance Measurements. *Z. Anorg. Allg. Chem.* **2011**, *637*, 1287–1294.
- (15) Brinkmann, D. NMR-Studies of Superionic Conductors. *Prog. Nucl. Magn. Reson. Spectrosc.* **1992**, *24*, 527–552.
- (16) Böhmer, R.; Jeffrey, K.; Vogel, M. Solid-state Li NMR with Applications to the Translational Dynamics in Ion Conductors. *Prog. Nucl. Magn. Reson. Spectrosc.* **2007**, *50*, 87–174.
- (17) Heitjans, P.; Schirmer, A.; Indris, S. In *Diffusion in Condensed Matter - Methods, Materials, Models*, 2nd ed.; Heitjans, P., Kärger, J., Eds.; Springer: Berlin, 2005; p 367.
- (18) Wilkening, M.; Lyness, C.; Armstrong, A. R.; Bruce, P. G. Diffusion in Confined Dimensions:  $\text{Li}^+$  Transport in Mixed Conducting  $\text{TiO}_2$ -B Nanowires. *J. Phys. Chem. C* **2009**, *113*, 4741–4744.
- (19) Wilkening, M.; Küchler, W.; Heitjans, P. From Ultra-slow to Fast Lithium Diffusion in the 2D Ion Conductor  $\text{Li}_x\text{TiS}_2$  - Probed Directly by Stimulated-Echo NMR and Nuclear Magnetic Relaxation. *Phys. Rev. Lett.* **2006**, *96*, 065901/1–065901/4.
- (20) Wilkening, M.; Mühle, C.; Jansen, M.; Heitjans, P. Microscopic Access to Long-Range Diffusion Parameters of the Fast Lithium Ion Conductor  $\text{Li}_x\text{BiO}_6$  by Solid State  $^7\text{Li}$  Stimulated Echo NMR. *J. Phys. Chem. B* **2007**, *111*, 8691–8694.
- (21) Wilkening, M.; Heitjans, P. Li Jump Process in  $h\text{-Li}_{0.7}\text{TiS}_2$  Studied by Two-time  $^7\text{Li}$  Spin-alignment Echo NMR and Comparison with Results on Two-dimensional Diffusion from Nuclear Magnetic Relaxation. *Phys. Rev. B* **2008**, *77*, 024311/1–024311/13.
- (22) Wilkening, M.; Kuhn, A.; Heitjans, P. Atomic-scale Measurement of Ultraslow Li Motions in Glassy  $\text{LiAlSi}_2\text{O}_6$  by Two-time  $^6\text{Li}$  Spin-alignment Echo NMR. *Phys. Rev. B* **2008**, *78*, 054303/1–054303/9.
- (23) Rao, R. P.; Adams, S. Studies of Lithium Argyrodite Solid Electrolytes for All-solid-state Batteries. *Phys. Status Solidi A* **2011**, *208*, 1804–1807.
- (24) Boulineau, S.; Courty, M.; Tarascon, J.-M.; Viallet, V. Mechanochemical Synthesis of Li-argyrodite  $\text{Li}_6\text{PS}_5\text{X}$  (X = Cl, Br, I) as Sulfur-based Solid Electrolytes for all Solid State Batteries Application. *Solid State Ionics* **2012**, *221*, 1.
- (25) Kuhn, A.; Sreeraj, P.; Pöttgen, R.; Wiemhöfer, H.-D.; Wilkening, M.; Heitjans, P. Li Ion Diffusion in the Anode Material  $\text{Li}_{12}\text{Si}_7$ : Ultrafast Quasi-1D Diffusion and Two Distinct Fast 3D Jump Processes Separately Revealed by  $^7\text{Li}$  NMR Relaxometry. *J. Am. Chem. Soc.* **2011**, *133*, 11018–11021.
- (26) Fukushima, E.; Roeder, S. B. W. *Experimental Pulse NMR*; Addison-Wesley: Reading, 1981.
- (27) Ailion, D.; Slichter, C. P. Study of Ultraslow Atomic Motions by Magnetic Resonance. *Phys. Rev. Lett.* **1964**, *12*, 168–171.
- (28) Slichter, C. P.; Ailion, D. Low-Field Relaxation and the Study of Ultraslow Atomic Motions by Magnetic Resonance. *Phys. Rev. B* **1964**, *135*, A1099–A1110.
- (29) Wilkening, M.; Epp, V.; Feldhoff, A.; Heitjans, P. Tuning the Li Diffusivity of Poor Ionic Conductors by Mechanical Treatment: High Li Conductivity of Strongly Defective  $\text{LiTaO}_3$  Nanoparticles. *J. Phys. Chem. C* **2008**, *112*, 9291–9300.
- (30) Wilkening, M.; Bork, D.; Indris, S.; Heitjans, P. Diffusion in Amorphous  $\text{LiNbO}_3$  Studied by  $^7\text{Li}$  NMR — Comparison with the Nano- and Microcrystalline Material. *Phys. Chem. Chem. Phys.* **2002**, *4*, 3246–3251.
- (31) Bertermann, R.; Müller-Warmuth, W.; Jansen, C.; Hiltmann, F.; Krebs, B. NMR Studies of the Lithium Dynamics in Two Thioborate Superionic Conductors:  $\text{Li}_9\text{B}_{19}\text{S}_{33}$  and  $\text{Li}_{4-2x}\text{Sr}_{2+x}\text{B}_{10}\text{S}_{19}$  ( $x \approx 0.27$ ). *Solid State Ionics* **1999**, *117*, 245–255.
- (32) Epp, V.; Gün, O.; Deiseroth, H.-J.; Wilkening, M. Long-range  $\text{Li}^+$  Dynamics in the Lithium Argyrodite  $\text{Li}_7\text{PSe}_6$  as Probed by Rotating-frame Spin-lattice Relaxation NMR. *Phys. Chem. Chem. Phys.* **2013**, *15*, 7123–7132.
- (33) Koch, B. Festkörper-NMR-Studien zur Struktur und Kationenmobilität in kristallinen Lithiumionenleitern. Ph.D. Thesis, University of Münster, Münster, 2009.
- (34) Wilkening, M.; Heitjans, P. From Micro to Macro: Access to Long-Range  $\text{Li}^+$  Diffusion Parameters in Solids via Microscopic  $^6,7\text{Li}$  Spin-Alignment Echo NMR Spectroscopy. *ChemPhysChem* **2012**, *13*, 53–65.
- (35) Note that with the NMR cryo probe employed we could not reach locking frequencies lower than 40 kHz. As can be seen from Figure 2, in the case of 3D BPP-type behavior a slight decrease in the locking frequency does influence the low- $T$  flank only. The peak maximum is expected to shift only slightly towards lower  $T$ . Even in the case of 45 kHz it is still expected to show up well below 200 K.
- (36) Bloembergen, N.; Purcell, E. M.; Pound, R. V. Relaxation Effects in Nuclear Magnetic Resonance Absorption. *Phys. Rev.* **1948**, *73*, 679–712.
- (37) Küchler, W.; Heitjans, P.; Payer, A.; Schöllhorn, R.  $^7\text{Li}$  NMR Relaxation by Diffusion in Hexagonal and Cubic  $\text{Li}_x\text{TiS}_2$ . *Solid State Ionics* **1994**, *70*, 434–438.
- (38) Mehrer, H. *Diffusion in Solids: Fundamentals, Methods, Materials, Diffusion-Controlled Processes*; Springer: Berlin, 2007.
- (39) Pecher, O.; Kong, S.-T.; Goebel, T.; Nickel, V.; Weichert, K.; Reiner, C.; Deiseroth, H.-J.; Maier, J.; Haarmann, F.; Zahn, D. Atomistic Characterisation of  $\text{Li}^+$  Mobility and Conductivity in  $\text{Li}_{7-x}\text{PS}_{6-x}\text{I}_x$  Argyrodites from Molecular Dynamics Simulations, Solid-State NMR, and Impedance Spectroscopy. *Chem.—Eur. J.* **2010**, *16*, 8347–8354.
- (40) *Diffusion in Condensed Matter - Methods, Materials, Models*, 2nd ed.; Heitjans, P., Kärger, J., Eds.; Springer: Berlin, 2005.
- (41) Winter, R.; Siegmund, K.; Heitjans, P. Nuclear Magnetic and Conductivity Relaxations by Li Diffusion in Glassy and Crystalline  $\text{LiAlSi}_4\text{O}_{10}$ . *J. Non-Cryst. Solids* **1997**, *212*, 215–224.
- (42) Bloembergen, N.; Purcell, E. M.; Pound, R. V. Relaxation Effects in Nuclear Magnetic Resonance Absorption. *Phys. Rev.* **1948**, *73*, 679–712.
- (43) Abragam, A. *The Principles of Nuclear Magnetism*; Clarendon: Oxford, U.K., 1961.
- (44) Wilkening, M.; Iwaniak, W.; Heine, J.; Epp, V.; Kleinert, A.; Behrens, M.; Nuspl, G.; Bensch, W.; Heitjans, P. Microscopic Li Self-diffusion Parameters in the Lithiated Anode Material  $\text{Li}_{4+x}\text{Ti}_5\text{O}_{12}$  ( $0 < x < 3$ ) Measured by  $^7\text{Li}$  Solid State NMR. *Phys. Chem. Chem. Phys.* **2007**, *9*, 6199–6202.
- (45) Meyer, M.; Maass, P.; Bunde, A. Spin-Lattice Relaxation: Non-Bloembergen-Purcell-Pound Behavior by Structural Disorder and Coulomb Interactions. *Phys. Rev. Lett.* **1993**, *71*, 573.
- (46) Bunde, A.; Dieterich, W.; Maass, P.; Meyer, M. In *Diffusion in Condensed Matter - Methods, Materials, Models*; Heitjans, P., Kärger, J., Eds.; Springer: Berlin, 2005; p 813.
- (47) Pietrass, T.; Taulelle, F.; Lavela, P.; OlivierFourcade, J.; Jumas, J. C.; Steuarnagel, S. Structure and Dynamics of Lithium-intercalated  $\text{SnS}_2$ .  $^6\text{Li}$ ,  $^7\text{Li}$  and  $^{119}\text{Sn}$  Solid State NMR. *J. Phys. Chem. B* **1997**, *101*, 6715–6723.
- (48) Wang, Z.; Gobet, M.; Sarou-Kanian, V.; Massiot, D.; Bessada, C.; Deschamps, M. Lithium Diffusion in Lithium Nitride by Pulsed-field Gradient NMR. *Phys. Chem. Chem. Phys.* **2012**, *14*, 13535–13538.

(49) Prasada Rao, R.; Sharma, N.; Peterson, V. K.; Adams, S. Formation and Conductivity Studies of Lithium Argyrodite Solid Electrolytes Using *in-situ* Neutron Diffraction. *Solid State Ion.* **2013**, *230*, 72–76.